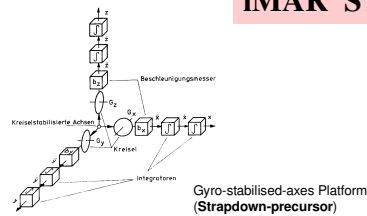
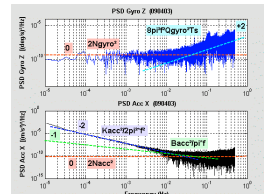
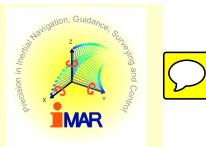


iMAR STRAPDOWN SURVEYING-GRADE IMU Type iNAV-RQH

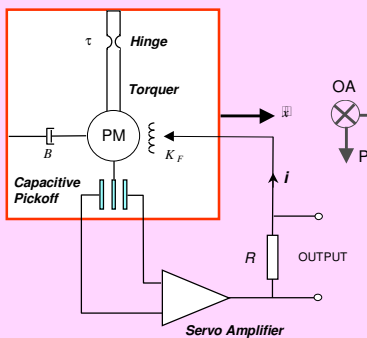


Dr. Raul Dorobantu¹, Dr. Christian Gerlach¹
Dr. Edgar von Hinüber², Dipl.-Ing. Markus Petry²

- Institut für Astronomische und Physikalische Geodäsie, Technische Universität München, Germany
raul@alpha.fsg.tu-muenchen.de, gerlach@bv.tum.de
- iMAR Solutions for Inertial Navigation and Surveying, St. Ingbert, Germany
y.hinuer@imar-navigation.de, m.petry@imar-navigation.de

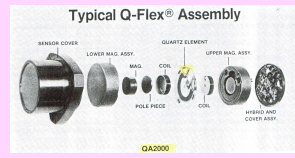
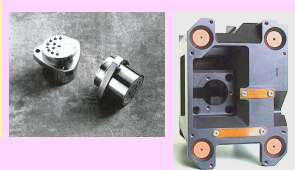


The QA2000 pendulous accelerometers are of force-rebalance type and show very good linearity and sensitivity. The capacitive pickoff commands the feedback system, to maintain the pendular arm as close as possible to the null position. The output signal (IMU's accelerometer output in [m/s²]) is proportional to the amplitude of the compensation current. The exploded view shows the quartz hinge as well as the electromagnetic torquer (Lorentz force).

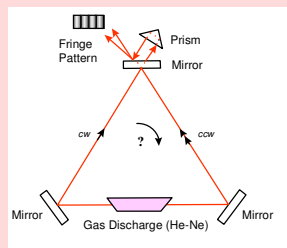


Accelerometer-triad error model:

$$\mathbf{f}_{out}^b = (\alpha SCF^T \cdot \mathbf{I} + \delta \alpha SCF + \delta \alpha MA) \cdot \mathbf{f}_{in}^b + \delta \mathbf{b}_{acc} + \delta \mathbf{n}_{acc} + \mathbf{v}_{acc}$$

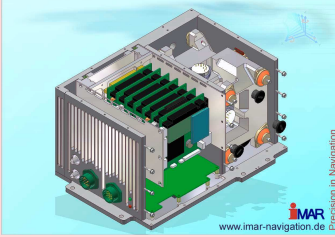


The RLG's (Ring Laser Gyroscope) working principle is based on the pure relativistic Sagnac effect. Two Laser waves, excited by a He-Ne gas discharging, are propagating in opposite directions in the resonance cavity. A rotation of the whole system results in frequency deviations. The displacement velocity of the fringe pattern (obtained from the interference of the two progressive waves) is proportional to the gyroscope rotation rate (IMU's output rate in [deg/s]).



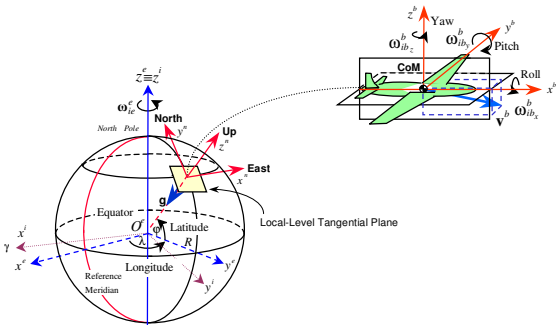
Gyroscope-triad error model:

$$\omega_{out}^b = (g SCF^T \cdot \mathbf{I} + \delta g SCF + \delta g MA) \cdot \omega_{in}^b + \delta \mathbf{b}_{gyro} + \delta \mathbf{n}_{gyro} + \delta g \mathbf{k}_{acc} + \mathbf{v}_{gyro}$$



A laboratory calibration of the IMU (Inertial Measurement Unit) was carried out on a rotating table. The gravity and the earth rotation vectors are used as reference for static calibration. A dynamical calibration can be done using a strapdown-navigation program.

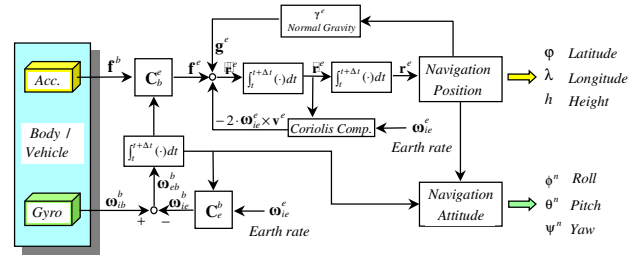
Relations between the operating inertial-, earth-, navigation- and body-frames.



The reference navigation system is the ENU local-level (East, North, Up).

The vehicle attitude – angular relations between the body system and the ENU reference - is continuously computed from the gyroscopic data.

The navigation solution is usually computed in ECEF (Earth Centered Earth Fixed) frame and transformed into the ENU frame (see e.g. the GPS/INS navigation program KINGSPAD, originating from the Calgary University). In comparison to an inertially-stabilized-axes platform, the strapdown measurement unit computes continuously the vehicle/IMU attitude, permitting the proper integration/compensation of the inertial data.



DGPS/INS Navigation Experiment

The navigation experiment made in Munich, on the Theresienwiese (an area with ideal GPS visibility), uses the carrier-phase DGPS trajectory solution as reference to put into evidence the positioning precision in the following settings:
INS only without any updating
INS only with ZUPTs
GPS/INS integration
INS only after GPS updating
The experiment shows the good navigation precision performance of the IMU (GPS/INS integrated solution with 1-sigma differences to the reference trajectory inferior to 0.3 cm and maximal values lower as 2.5 cm). Through their positioning, attitude and acceleration performance, the IMU can be considered appropriate also for high precision gravity determination missions.

$$\begin{bmatrix} \dot{\delta \mathbf{e}}^e \\ \dot{\delta \mathbf{v}}^e \\ \dot{\delta \mathbf{a}}^e \\ \dot{\delta \mathbf{b}} \end{bmatrix} = \begin{bmatrix} -\mathbf{F}^e \mathbf{e}^e + \mathbf{N}^e \delta \mathbf{e}^e - 2\Omega_{ie}^e \delta \mathbf{v}^e + \mathbf{C}_b^e \mathbf{b} \\ -\Omega_{ie}^e \mathbf{e}^e + \mathbf{C}_b^e \mathbf{d} \\ -\kappa \mathbf{d} + \mathbf{w}_d \\ -\beta \mathbf{b} + \mathbf{w}_b \end{bmatrix}$$

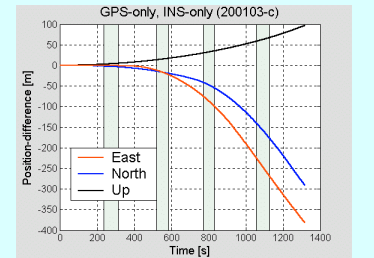
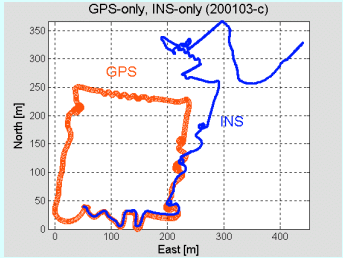
The 15-variables Kalman filter error state equations, used in the Kingspad software, is given here in vectorial form. This stochastic filter permits an optimal estimation of state errors. The left vectorial column represents the error states derivatives of positions, velocities and attitude angles, respectively. All of them are expressed in the e-frame. The last two vectors are the time-derivatives of the rate, resp. accelerometer bias-offsets (modelled as stochastic Gauss-Markov noise processes).

$$\delta Position_{bias_{acc}} = \frac{1}{2} \delta b_{acc} \cdot t^2$$

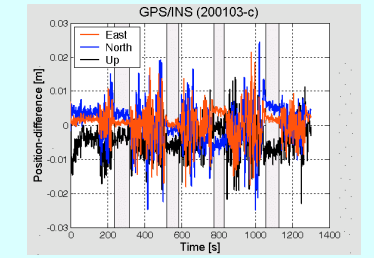
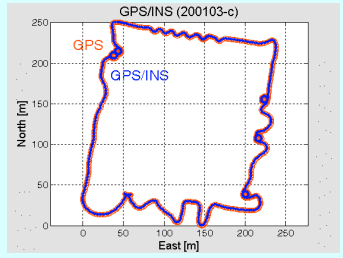
$$\delta Position_{bias_{gyro}} = \frac{1}{6} g \cdot \delta b_{gyro} \cdot t^3$$

The parabolic shape of the position errors shows some quadratic and cubic dependencies (see the experiment results), which could be put into relation to elementary integration processes (which consider only the residual bias-offsets in a simplified compensating model).

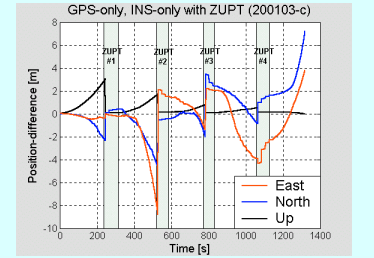
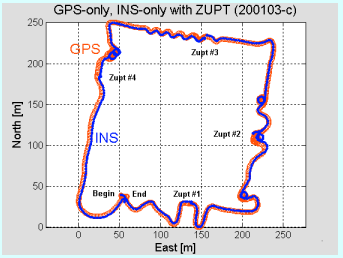
The INS-only solution, without any update, shows a great discrepancy from the reference DGPS trajectory, in the range of hundreds of meters. This is due to the permanent accumulation of positioning errors, caused principally by the integration of the residual inertial sensor errors. The right diagram shows the uncompensated navigation errors (differences to the DGPS reference trajectory).



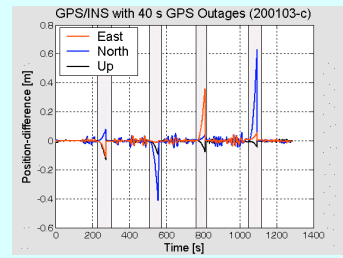
For the completeness of the evaluation, an integrated DGPS/INS solution has been computed, with GPS updates every second. The results – trajectory and differences in comparison to the DGPS reference solution – shows errors (differences) with sub-centimeter 1-sigma values (e.g., as low as 0.003 m for the vertical channel, which, in addition, was bias-compensated). Of course, essentially lower values are present during the stationary ZUPT periods.



To improve the uncompensated INS-only solution (see above) we introduced four zero velocity updates (ZUPT) in the computation of the navigation solution. This is a common practice in geodetic applications with no GPS update possibilities (like e.g. tunnel surveying). The evident INS-only trajectory precision improvement due to only four ZUPTs is shown below. The characteristic Kalman filter learning process is best illustrated for the vertical channel (right figure): one observes the diminishing of the time-accumulated errors after every ZUPT.



Simulation results for 40 s GPS outages, produced during stationary periods of the vehicle (however, after a GPS/INS integratio/calibration period) shows, e.g., for the z-axis accelerometer - additionally corrected for a bias-offset – quite low differences, which don't exceed the value of 15 cm.



A measure for the precision of the kinematic DGPS solution is given by comparing the known fixed distance of 1.40 m between the two rover-antennas (see the red line) with the DGPS solution for the same distance. The standard deviation of the relative position error for the two rover antennas don't exceed 0.27 cm.

